

QNLP in Practice: Running Compositional Models of Meaning on a Quantum Computer

Robin Lorenz[†] Anna Pearson[†] Konstantinos Meichanetzidis^{†‡}
Dimitri Kartsaklis[†] Bob Coecke[†]

[†]Cambridge Quantum Computing [‡]University of Oxford

{robin.lorenz;anna.pearson;k.mei;dimitri.kartsaklis;
bob.coecke}@cambridgequantum.com

Abstract

Quantum Natural Language Processing (QNLP) deals with the design and implementation of NLP models intended to be run on quantum hardware. In this paper, we present results on the first NLP experiments conducted on Noisy Intermediate-Scale Quantum (NISQ) computers for datasets of size ≥ 100 sentences. Exploiting the formal similarity of the compositional model of meaning by Coecke et al. (2010) with quantum theory, we create representations for sentences that have a natural mapping to quantum circuits. We use these representations to implement and successfully train two NLP models that solve simple sentence classification tasks on quantum hardware. We describe in detail the main principles, the process and challenges of these experiments, in a way accessible to NLP researchers, thus paving the way for practical Quantum Natural Language Processing.

1 Introduction

Bringing the promise of computational speeds exponentially higher than the current standard, quantum computing is rapidly evolving to become one of the most popular cutting-edge areas in computer science. And while, until recently, most of the work in quantum computing was purely theoretical or concerned with simulations on classical hardware, the advent of the first quantum computers available to researchers, referred to as *Noisy Intermediate-Scale Quantum* (NISQ) devices, has already led to some promising practical results and applications spanning a wide range of topics such as cryptography (Pirandola et al., 2020), chemistry (Cao et al., 2019), and biomedicine (Cao et al., 2018).

An obvious question is whether this new paradigm of computation can also be used for NLP. Such applicability may be to the end of leveraging the computational speed-ups for language-related problems, as well as for investigating how quantum systems, their mathematical description and

the way information is encoded “quantumly” may lead to conceptual and practical advances in representing and processing language meaning beyond computational speed-ups.

Inspired by these prospects, *quantum natural language processing* (QNLP), a field of research still in its infancy, aims at the development of NLP models explicitly designed to be executed on quantum hardware. There exists some impressive theoretical work in this area, but the proposed experiments are classically simulated. A notable exception to this is recent work by two of the authors (Meichanetzidis et al., 2020), where a proof of concept experiment of very small scale was performed on quantum hardware for the first time.

Following and adding to the ideas and results of that work, in this paper we present two complete medium-scale experiments consisting of linguistically-motivated NLP tasks running on quantum hardware. The goal of these experiments is not to demonstrate some form of “quantum advantage” over classical implementations in NLP tasks; we believe this is not yet possible due to the limited capabilities of currently available quantum computers. In this work, we are mostly interested in providing a detailed account to the NLP community of what QNLP entails in practice. We show how the traditional modelling and coding paradigm can shift to a quantum-friendly form, and we explore the challenges and limitations imposed by the current NISQ computers.

From an NLP perspective, both tasks involve some form of sentence classification: for each sentence in the dataset, we use the compositional model of Coecke et al. (2010) – often dubbed as DISCOCAT (DIStributIonal COmpositional CATegorical) – to compute a state vector, which is then converted to a binary label. The model is trained on a standard binary cross entropy objective, using an optimisation technique known as *Simultaneous Per-*

turbation Stochastic Approximation (SPSA). The results obtained from the quantum runs are accompanied by various classical simulations which show the projected long-term behaviour of the system in the absence of hardware limitations.

The choice of DISCOCAT is motivated by the fact that the derivations it produces essentially form a tensor network, which means they are already very close to how quantum computers process data. Furthermore, the model comes with a rigorous treatment of the interplay between syntax and semantics and with a convenient diagrammatic language. In Section 5 we will see how the produced diagrams get a natural translation to quantum circuits – the basic units of computation on a quantum computer¹ – and how sentences of different grammatical structure are mapped to different quantum circuits. We will also explain how tensor contraction (the composition function) has its expression in terms of quantum gates. We further discuss the role of noise on a NISQ device, and how this affects our designing choices for the circuits. The experiments are performed on an IBM NISQ computer provided by the IBM Quantum Experience platform².

For our experiments we use two different datasets. The first one (130 sentences) is generated automatically by a simple context-free grammar, with half of the sentences related to food and half related to IT (a binary classification task). The other one (105 noun phrases) is extracted from the RELPRON dataset (Rimell et al., 2016), and the goal of the model is to predict whether a noun phrase contains a subject-based or an object-based relative clause (again a binary classification task). We demonstrate that the models converge smoothly, and that they produce good results (given the size of the datasets) in both quantum and simulated runs.

In summary, the contributions of this paper are the following: firstly, we outline in some depth the process, the technicalities and the challenges of training and running an NLP model on a quantum computer; secondly, we provide a strong proof of concept that quantum NLP is in our reach.

The structure of the paper is the following: Section 2 discusses the most important related work on experimental quantum computing and QNLP; Section 3 describes DISCOCAT; Section 4 provides an introduction to quantum computing; Section 5 gives a high-level overview for a general QNLP pipeline; Section 6 explains the tasks; Section 7 pro-

¹In the circuit-based, as opposed to the measurement-based, model of quantum computation.

²<https://quantum-computing.ibm.com>

vides all the necessary details for the experiments and finally; Section 8 summarises our findings and points to future work.

2 Related work

There is a plethora of hybrid classical-quantum algorithms with NISQ technology in mind (Bharti et al., 2021). The majority of already implementable quantum machine learning (QML) protocols are based on *variational quantum circuit* methods (Benedetti et al., 2019). However, useful quantum algorithms with theoretically proven speedups assume fault-tolerant quantum computers, which are currently not available. (See Section 4 for more details.)

In the context of compositional QNLP, there is the early theoretical work by Zeng and Coecke (Zeng and Coecke, 2016), in which the DISCOCAT model³ is leveraged to obtain a quadratic speedup. Further theoretical work (Coecke et al., 2020) lays the foundations for implementations on NISQ devices. In (O’Riordan et al., 2020), a DISCOCAT-inspired workflow was introduced along with experimental results obtained by classical simulation. Regarding parsing, in (Bausch et al., 2020) the authors employ Grover search to achieve super-polynomial speedups, while Wiebe et al. (2019) use quantum annealing to solve problems for general context-free languages. In (Gallego and Orus, 2019), parse trees are interpreted as information-coarse-graining tensor networks where it is also proposed that they can be instantiated as quantum circuits. Ramesh and Vinay (2003) provide quantum speedups for string-matching which is relevant for language recognition. We also mention work on quantum-inspired classical models incorporating features of quantum theory such as its inherent probabilistic nature (Basile and Tamburini, 2017) or the existence of many-body entangled states (Chen et al., 2020). Finally, although not directly related to NLP, there is a lot of interesting work on quantum neural networks, see for example (Gupta and Zia, 2001; Beer et al., 2020).

Recently, Meichanetzidis et al. (2020) provided for the first time a proof of concept that practical QNLP is in principle possible in the NISQ era, by managing to run and optimize on a NISQ device a classifier using a dataset of 16 artificial short sentences. The current work is a natural next step, presenting for the first time two NLP experiments of medium scale on quantum hardware.

³For an introduction to DISCOCAT, see Section 3.

3 A model of meaning inspired by quantum mechanics

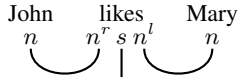
Based on the rigorous mathematical framework of compact closed categories, the DISCOCAT model of Coecke et al. (2010) is of particular interest for our purposes, since its underlying compact-closed structure provides an abstraction of the Hilbert space formulation of quantum theory (Abramsky and Coecke, 2004). In this model, the meaning of words is represented by tensors whose order is determined by the types of words, expressed in a *pregroup grammar* (Lambek, 2008). A type p has a left (p^l) and a right adjoint (p^r), and the grammar has only two reduction rules:

$$p \cdot p^r \rightarrow 1 \quad p^l \cdot p \rightarrow 1 \quad (1)$$

Assuming atomic types n for nouns and noun phrases and s for sentences, the type of a transitive verb becomes $n^r \cdot s \cdot n^l$, denoting that an n is expected on the left and another one on the right, to return an s . Thus, the derivation for a transitive sentence such as “John likes Mary” gets the form:

$$n \cdot (n^r \cdot s \cdot n^l) \cdot n \rightarrow (n \cdot n^r) \cdot s \cdot (n^l \cdot n) \rightarrow 1 \cdot s \cdot 1 \rightarrow s \quad (2)$$

showing that this is a grammatical sentence. In diagrammatic form:



where the “cups” (\cup) denote the grammar reductions. The transition from pregroups to vector space semantics is achieved by a mapping⁴ \mathcal{F} that sends atomic types to vector spaces (n to N and s to S) and composite types to tensor product spaces ($n^r \cdot s \cdot n^l$ to $N \otimes S \otimes N$). For example, a transitive verb becomes a tensor of order 3, which can be seen as a bilinear map $N \otimes N \rightarrow S$, while an adjective (with type $n \cdot n^l$) can be seen as a matrix, representing a linear map $N \rightarrow N$. Further, \mathcal{F} translates all grammar reductions to tensor contractions, so that the meaning of a sentence $s = w_1 w_2 \dots w_n$ with a pregroup derivation α is given by:

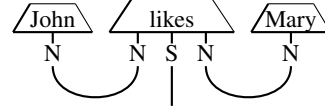
$$s = \mathcal{F}(\alpha) [\mathbf{w}_1 \otimes \mathbf{w}_2 \otimes \dots \otimes \mathbf{w}_n] \quad (3)$$

Here, \mathcal{F} turns α into a linear map that, applied to the tensor product of the word representations, by tensor-contracting that expression returns a vector for the whole sentence. As a concrete example, the meaning of the sentence “John likes Mary”

⁴This mapping can be formalised as a category-theoretic functor (Kartsaklis et al., 2016).

becomes $s = \mathbf{j} \cdot \mathbf{L} \cdot \mathbf{m}$, where $\mathbf{j}, \mathbf{m} \in N$ and $\mathbf{L} \in N \otimes S \otimes N$. Above, \mathbf{L} is a tensor of order 3, and s is a vector in S . Note that the underlying field of the vector spaces is not specified, and can, e.g., be \mathbb{R} or \mathbb{C} depending on the particular type of model (it is \mathbb{C} in this work).

Meaning computations like the example above can be conveniently represented using the diagrammatic calculus of compact closed categories (Coecke and Kissinger, 2017):



where the boxes denote tensors, the order of which is determined by the number of their wires, while the cups are now the tensor contractions. Note the similarity between the pregroup diagram above with the one here, and how the grammatical derivation essentially dictates both the shapes of the tensors and the contractions. As we will see later, these *string diagrams* can further naturally be mapped to quantum circuits, as used in quantum computation.

There is a rich literature on the DISCOCAT model, and here we mention only a few indicative publications. Proposals for modelling verbs and implementations of the model have been provided by Grefenstette and Sadrzadeh (2011) and Kartsaklis et al. (2012); Kartsaklis and Sadrzadeh (2014). Sadrzadeh et al. (2013) address the modelling of relative pronouns. Piedeleu et al. (2015) present a version of the model where the meaning of words is given by density matrices, encoding phenomena such as homonymy and polysemy. Finally, versions of the model have been used extensively in conceptual tasks such as textual entailment at the level of sentences, see for example (Sadrzadeh et al., 2018; Bankova et al., 2019; Lewis, 2019).

4 Introduction to quantum computing

For any serious introduction into quantum information theory and quantum computing, which obviously is beyond the scope of this paper, the reader is referred to the literature (see, e.g., Refs. Coecke and Kissinger (2017) and Nielsen and Chuang (2011)). However, for the sake of a self-contained manuscript, this section will, in a pragmatic way and with a reader in mind who has had no exposure to quantum theory, set out the required terms and concepts.

We naturally start with a *qubit*, which, as the

most basic unit of information carrier, is the quantum analogue of a bit, and yet a very different sort of thing. It is associated with a property of a physical system such as the spin of an electron (‘up’ or ‘down’ along some axis), and has a *state* $|\psi\rangle$ that lives in a 2-dimensional *complex* vector space (more precisely a Hilbert space). With $|0\rangle$, $|1\rangle$ denoting orthonormal basis vectors,⁵ which are related to the respective outcomes ‘0’ and ‘1’ of a measurement, a general state of the qubit is a linear combination known as a *superposition*: $|\psi\rangle = \alpha|0\rangle + \beta|1\rangle$, where $\alpha, \beta \in \mathbb{C}$ and $|\alpha|^2 + |\beta|^2 = 1$.

Importantly, quantum theory is a *fundamentally probabilistic* theory, that is, even given that a qubit is in state $|\psi\rangle$ – a state known as perfectly as is in principle possible – this generally allows one only to make predictions for the probabilities, with which the outcomes ‘0’ and ‘1’, respectively, occur when the qubit is *measured*. These probabilities are given by the so-called Born rule $P(i) = |\langle i|\psi\rangle|^2$, where $i = 0, 1$ and the complex number $\langle i|\psi\rangle$, called the *amplitude*, is given by the inner product written as the composition of state $|\psi\rangle$ with *quantum effect* $\langle i|$. Hence, for the above state, $P(0) = |\alpha|^2$ and $P(1) = |\beta|^2$.

The evolution of an isolated qubit before measuring it is described through the *transformation* of its state with a *unitary* linear map U , i.e. $|\psi'\rangle = U|\psi\rangle$. See Fig. 1a for a diagrammatic representation of such evolution.

The joint state space of q qubits is given by the tensor product of their individual state spaces and thus has (complex) dimension 2^q . For instance, for two ‘uncorrelated’ qubits in states $|\psi_1\rangle = \alpha_1|0\rangle + \beta_1|1\rangle$ and $|\psi_2\rangle = \alpha_2|0\rangle + \beta_2|1\rangle$, the joint state is $|\psi_1\rangle \otimes |\psi_2\rangle$, which in basis-dependent notation becomes $(\alpha_1, \beta_1)^T \otimes (\alpha_2, \beta_2)^T = (\alpha_1\alpha_2, \alpha_1\beta_2, \beta_1\alpha_2, \beta_1\beta_2)^T$. The evolution of a set of qubits that interact with each other, is described by a unitary map acting on the overall state space. The diagrammatic representation from Fig. 1a then extends correspondingly to a *quantum circuit*, such as the example shown in Fig. 1b.

On the one hand, such a quantum circuit captures the structure of the overall linear map evolving the respective qubits, where parallel ‘triangles’ and parallel boxes are to be read as tensor products of

⁵We use Dirac (bra-ket) notation, where the ‘bra’, also called the effect, $\langle\phi|$ is the dual vector of the ‘ket’ $|\phi\rangle$, the state. States are representable as column vectors and effects as row vectors.

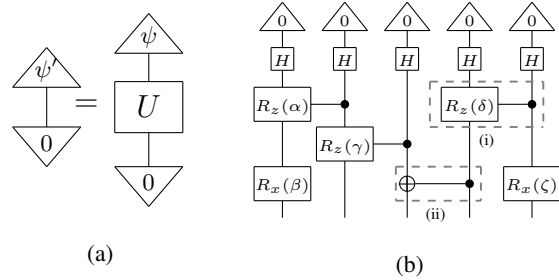


Figure 1: (a) Basic example of the diagrammatic representation, here of $\langle 0|\psi'\rangle = \langle 0|U|\psi\rangle$, i.e. the evolution of a qubit in initial state $|\psi\rangle$ with unitary map U and then composed with the effect $\langle 0|$, corresponding to the (non-deterministic) outcome ‘0’. (b) Example of a quantum circuit, which contains all the kinds of gates relevant to this paper: the Hadamard gate H , the X-rotation gate $R_x(\beta)$ by angle β , the controlled Z-rotation gate (i), a component of which is a Z-rotation gate $R_z(\delta)$ by angle δ , and finally the quantum CNOT gate (ii).

states and unitary maps, respectively, and sequential ‘wiring up’ of boxes as composition of linear maps. Hence, a circuit as a whole represents the application of a linear map to a vector, computing the systems’ overall state at a later time – in other words, it is simple linear algebra and can be viewed as tensor contraction of complex valued tensors that are represented by the gates.

On the other hand, a circuit can conveniently also be seen as a list of abstract instructions for what to actually *implement* on some quantum hardware in order to make, say, some photons⁶ undergo, physically, the corresponding transformations as prescribed by the gates of the circuit.

Now, coming back to the fact that quantum theory is probabilistic, once a circuit has been run on hardware all qubits are measured. In the case of Fig. 1b this yields 5 bits each time and many such runs have to be repeated to obtain statistics from which to estimate the outcome probabilities. These probabilities connect theory and experiment.

In order to obtain the result for a given problem, the design of the circuit has to encode the problem such that that result is a function of the outcome probabilities. Hence, the choice of circuit is key.

A special case, albeit straightforward, is worth mentioning due to its relevance for this paper: the encoding of the quantity of interest in a circuit over, say, q qubits may be such that the result is a function of the outcome distribution on just r of the

⁶The basic physical object used as a qubit varies vastly across different quantum computers.

qubits ($r < q$), but subject to the condition that the remaining $q - r$ qubits have yielded particular outcomes, i.e. the result is a function of the corresponding conditional probability distribution. The technical term for this is *post-selection*, seeing as one has to run the whole circuit many times and measure all qubits to then restrict – post-select – the data for when the condition on the $q - r$ qubits is satisfied. At the diagrammatic level the need for such post-selection is typically indicated by the corresponding quantum effects as done, e.g., in Fig. 5, which up to the 0-effects on 4 of the 5 qubits, is identical to that of Fig. 1b.

Usually, the power of quantum computing is naively attributed to ‘quantum parallelism’; that one can create exponentially large superpositions over the solution space of a problem. However, the caveat, and the reason why it is not believed that quantum computers can efficiently solve NP-complete problems, is that the output is a probability distribution one needs to sample from. Viewing quantum theory as a generalisation of probability theory, one realises that a key notion that quantum computing allows for is *interference*; amplitudes sum as complex numbers. Designing quantum algorithms amounts to crafting amplitudes so that the wrong solutions to a problem interfere destructively and the correct ones constructively so that they can be measured with high probability. This is a hard conceptual problem in itself, which explains the relatively small number of quantum algorithms, albeit very powerful ones, in the quantum computer scientist’s arsenal.

Actually building and running a quantum computer is a challenging engineering task for multiple reasons. Above all, qubits are prone to random errors from their environment and unwanted interactions amongst them. This ‘coherent noise’ is different in nature to that of a classical computing hardware. A quantum computer that would give the expected advantages for large scale problems, is one that comes with a large number of so called fault-tolerant qubits, essentially obtained by clever error correction techniques. Quantum error correction (Brown et al., 2016) reduces to finding ways for distributively encoding the state of a logical qubit on a large number of physical qubits (hundreds or even thousands). Their scalable technical realisability is still out of reach at the time of writing. The currently available quantum devices are rather noisy medium-scale machines with fewer than 100 physical qubits, playing mostly the role

of proof of concept and being extremely valuable assets for the development of both theory and applications. This is the reason one speaks of the NISQ era, mentioned in Sec. 1, and this is the light in which the experimental pioneering on QNLP presented in this paper has to be seen – exciting proof of concept, while the machines are still too small and noisy for large scale QNLP experiments.

5 The general pipeline

Section 4 explained that the quantum computing equivalent to classical programming involves the application of quantum gates on qubits according to a quantum circuit. This section explains the general pipeline of our approach, i.e. in particular the process of how to go from a sentence to its representation as a quantum circuit, on the basis of which the model predicts the label. Figure 2 schematically depicts this pipeline, each numbered step of which will be addressed subsequently at a generic level, whereas concrete examples of choices that one has to make along the way will be covered in the implementation of this pipeline presented in Sec. 7.

Since DISCOCAT is syntax-sensitive, the first step is to get a syntax tree corresponding to the sentence, on the basis of which a DISCOCAT derivation is created in a diagrammatic form. In order to avoid computational complications on quantum hardware, this diagram is first optimised to yield the input into an *ansatz* that then determines the actual conversion into a quantum circuit. A quantum compiler translates the latter into hardware-specific code that can be run on quantum hardware. These stages are described in more detail below.

Step 1: For a large-scale NLP experiment with thousands of sentences of various structures, the use of a pregroup parser for providing the syntax trees would be necessary.⁷ In the present

⁷Since to the best of our knowledge at the time of writing there are not any robust pregroup parsers available, an alterna-

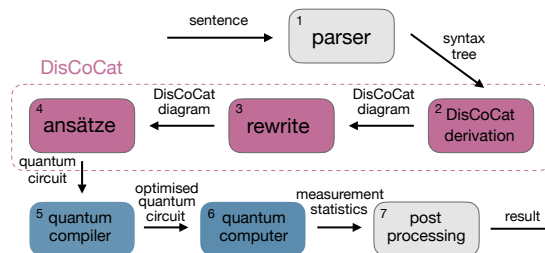


Figure 2: Schematic overview of the general pipeline.

work, though, this step can be executed semi-automatically due to the limited vocabulary and the small number of different grammatical structures in our sentences. For instance, with nouns, adjectives and transitive verbs having the respective types $n, n \cdot n^l$ and $n^r \cdot n \cdot n^l$, the sentence “person prepares tasty dinner” is parsed as below (see Sec. 3 for more details):

$$\begin{aligned} n \cdot (n^r \cdot s \cdot n^l) \cdot (n \cdot n^l) \cdot n &\rightarrow (n \cdot n^r) \cdot \\ s \cdot (n^l \cdot n) \cdot (n^l \cdot n) &\rightarrow 1 \cdot s \cdot 1 \cdot 1 \rightarrow s \end{aligned} \quad (4)$$

Step 2: Construct the sentences’ DisCoCat diagrams by representing each word as a state and then ‘wiring them up’ by drawing a cup for every reduction rule. The above example becomes:⁸

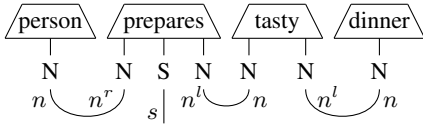


Figure 3

Step 3: The structure of compact closed categories comes with rewrite rules that allow the transformation of diagrams like the above into equivalent ones, which, depending on the final implementation, can bring computational advantages. While so far there is no universal recipe for how to do this optimally, one crucial observation in light of a quantum implementation is that cups are costly (see Step 5). One simple, but effective transition to equivalent diagrams is therefore achieved by ‘bending down’ all nouns of a sentence⁹ like ‘person’ and ‘dinner’ in the example:

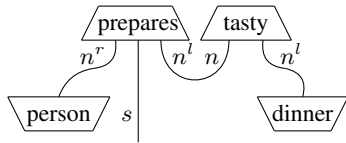


Figure 4

tive approach would be to use a CCG parser and subsequently convert the types into pregroups. This however comes with a few caveats, the discussion of which is outside the scope of this paper.

⁸As discussed in Sec. 3, the diagram in Fig. 3 represents linear-algebraic operations between tensors in vector spaces N, S and tensor products of them. For convenience, we also include the pregroup types as a reminder of the grammatical rules involved in each contraction. For the remainder of this paper, only the pregroup types will be shown since they are indicative of the vector spaces they are mapped to.

⁹Effectively replacing the cup and the noun’s state $1 \rightarrow n$ with an effect $n^r \rightarrow 1$ or $n^l \rightarrow 1$, depending on which end of the cup the noun was.

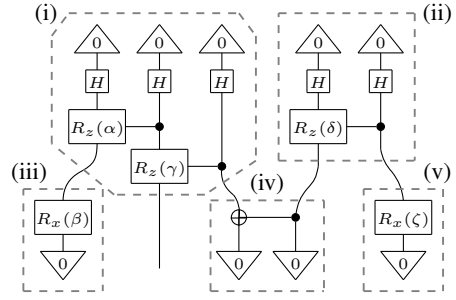


Figure 5: Example of interpreting Fig. 4 as a quantum circuit according to an ansatz. Here $q_n = 1 = q_s$, the words ‘prepares’ and ‘tasty’ replaced with the quantum states marked by (i) and (ii), respectively, ‘person’ and ‘dinner’ replaced with the quantum effects marked as (iii) and (v), respectively, and the cup written as the Bell effect in component (iv).

This way the number of cups is reduced by as many nouns as are present in the sentence.

Step 4: This is the step where the abstract DISCOCAT representation takes a more concrete form: the DISCOCAT diagram is mapped to a specific quantum circuit. This map is determined by: (a) choosing the number q_n and q_s of qubits that every wire of type n and s , respectively, as well as dual types thereof, get mapped to; and (b) choosing concrete parametrised quantum states (effects) that all word states (effects) get consistently replaced with. We refer to the conjunction of such choices as an *ansatz*. Note that each cup¹⁰ is equivalent to a *Bell-effect* (see Fig. 5). Principled approaches to (b) are presented in Sec. 7, but for an illustration consider the example from Fig. 4 translated into a quantum circuit of the form as shown in Fig. 5.

It is worth emphasising that the mapping’s output is a circuit whose connectivity is fixed by the sentence’s syntax, while the choice of ansatz determines the number of parameters for each word’s representation. Now, in principle it is of course known how many parameters p are needed to fix the most general state on q qubits, so why is this choice of ansatz important (independent from questions of overfitting and generalisation)? There are two reasons, which are both of a practical nature. First, p is exponential in q . So, even beyond the NISQ era, for the sort of dataset size and length of sentences one wishes to consider in NLP, a feasible number of parameters has to be achieved. Second, different quantum machines have different sets of ‘native’ gates, and some gates are less prone to errors than others when implemented. Hence, on

¹⁰Recall from the discussion in Sec. 3 that cups can also be seen to correspond to tensor contractions.

NISQ machines the choice of ansatz should be informed by the actual hardware to avoid unnecessary gate-depth after compilation and hence noise from mere re-parametrisation.

Step 5: A quantum compiler translates the quantum circuit into machine specific instructions. This includes expressing the circuit’s quantum gates in terms of those actually physically available on that machine and ‘routing’ the qubits to allow for the necessary interactions given the device’s topology, as well as an optimisation to further reduce noise.

Part of this step also is the necessary bookkeeping to do with post-selection (see Sec. 4). The 0-effects in Fig. 5, while crucial parts of the sentence’s representation, are not deterministically implementable operations; as outcomes of measurements, they are obtained only with a certain probability. The circuit corresponding to Fig. 5 that can be implemented, is hence precisely that of Fig. 1b with the additional operation of measuring all 5 qubits at the end. All that one has to do is remember which qubits, after many runs of the quantum circuit (these runs giving *shots*), have to be post-selected on the 0-outcome.

Here we see the reason for why cups are costly, since each cup leads to $2q_n$ (or $2q_s$) qubits that require post-selection. Had one stuck to the diagram in Fig. 3 then 6 out of 7 qubits would have had to be post-selected, rather than 4 out of 5 based on Fig. 4. With sentences just slightly longer than in the example and limited number n_{shots} of shots of any given circuit (2^{13} for IBM quantum devices) one easily runs into severe statistical limitations to reliably estimate the desired outcome probabilities.

Step 6: The quantum computer runs the circuit n_{shots} times, i.e. for each run prepares initial states, applies the gates and measures all the qubits at the end. This returns outcome counts of the shots for all qubits.

Step 7: Post-processing applies the above mentioned post-selection process and turns the counts into estimations of relative frequencies, which are the input into any further post-processing for the calculation of a task-specific final result.

6 The tasks

We define two simple binary classification tasks for sentences. In the first one, we generated sentences of simple syntactical forms (containing at most 5 words) from a fixed vocabulary by using a simple context-free grammar (Table 1). The nature of the vocabulary (of size 17) allowed us to choose

noun_phrase	→ noun
noun_phrase	→ adjective noun
verb_phrase	→ verb noun_phrase
sentence	→ noun_phrase verb_phrase

Table 1: Context-free grammar for the *MC* task.

sentences that look natural and refer to one of two possible topics, food or IT. The chosen dataset of this task, henceforth referred to as *MC* (‘meaning classification’), consists of 65 sentences from each topic, similar to the following:

“skillful programmer creates software”
“chef prepares delicious meal”

Part of the vocabulary is shared between the two classes, so the task (while still an easy one from an NLP perspective) is not trivial.

In a slightly more conceptual task, we select 105 noun phrases containing relative clauses from the RELPRON dataset (Rimell et al., 2016). The phrases are selected in such a way that each word occurs at least 3 times in the dataset, yielding an overall vocabulary of 115 words. While the original task is to map textual definitions (such as “device that detects planets”) to terms (“telescope”), for the purposes of this work we convert the problem into a binary-classification one, with the goal to predict whether a certain noun phrase contains a subject relative clause (“device that detects planets”) or an object relative clause (“device that observatory has”). Our motivation behind this task, henceforth referred to as *RP*, is that it requires some syntactic awareness from the model, so it is a very reasonable choice for testing DISCOCAT. Further, the size of vocabulary and consequently the sparseness of words make this task a much more challenging benchmark compared to the *MC* task.

These simple datasets already pose challenges in two ways. First, concerning the lengths of sentences (see Step 5 of Sec. 5 and also Sec. 8). Second, concerning the lengths of datasets, since they already reach the limits of the currently available quantum hardware – even just doubling the number of sentences would start to approach an unfeasible time cost given the shared available resources (more details about this in Sec. 7.4).

7 Experiments

The experiments reported in this paper address the two tasks *MC* and *RP*, respectively, by implementing the pipeline from Fig. 2 together with an optimisation procedure to train the model parameters

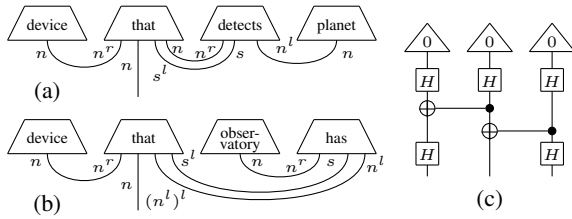


Figure 6: DISCoCAT diagrams for example phrases from the *RP* dataset, where in (a) ‘that’ is the subject, while in (b) it is the object. (c) depicts the quantum state (a GHZ state) assigned to ‘that’ as part of our ansätze, given that $q_n = 1$ and $q_s = 0$.

against an objective function, as in standard supervised machine learning. Importantly, training the model amounts to learning the word representations in a task-specific way, while all other aspects of the DISCoCAT model are dictated by syntax or are contingent hyperparameters that fix the ansatz. Our Python implementation¹¹ used the DISCOPY package¹² (de Felice et al., 2020) to implement the DISCoCAT specific Steps 2-4, the Python interface of the quantum compiler *t|ket*TM¹³ (Sivaramajah et al., 2020) for Step 5, and the IBM device `ibmq_bogota` for Step 6. The remainder of this section describes all steps in detail.

As the datasets of both tasks are simple, parsing can be done semi-automatically. For the noun phrases and sentences considered in this work, we simply note that relative pronouns in the subject case take pregroup type $n^r \cdot n \cdot s^l \cdot n$, while in the object case their type is $n^r \cdot n \cdot (n^l)^l \cdot s^l$, and we remind the reader that the types for adjectives and transitive verbs are, respectively, $n \cdot n^l$ and $n^r \cdot s \cdot n^l$. One can then refer to Step 2 in Sec. 5 to work out the derivations and convince oneself that they have a unique reduction to n or s . For illustration, diagrams (a) and (b) in Fig. 6 depict two noun phrases from the *RP* dataset, while the example in Fig. 3 is a sentence from the *MC* dataset. The scheme described in Step 3 of ‘bending the nouns’ was consistently applied to both datasets.

7.1 Parametrisation – the ansätze

As explicated in Sec. 5, Step 4, the choice of ansatz determines the parametrisation of the concrete family of models. We studied a variety of ansätze for

¹¹The Python code and the datasets will be made available at https://github.com/CQCL/qnlp_lorenz_et_al_2021_resources.

¹²<https://github.com/oxford-quantum-group/discopy>

¹³<https://github.com/CQCL/pytket>

both tasks. For each ansatz all appearing parameters are valued in $[0, 2\pi]$.

In order to keep the number of qubits as low as possible in light of the noise in NISQ devices, while having at least one qubit to encode the label – we are trying to solve a binary classification task after all – we set $q_n = 1$ and $q_s = 1$ for the *MC* task, but $q_s = 0$ for the *RP* task (noting that the type of the phrases here is n). Recall that the vector spaces in which the noun and sentence embeddings live have (complex) dimension $N = 2^{q_n}$ and $S = 2^{q_s}$, respectively.

Due to our scheme from Step 3 (see Sec. 5) all nouns appear as effects $\langle w|$, for which two options were considered (always consistently applied to all nouns of the dataset). First, an Euler decomposition that involves three parameters and assigns $\langle w| = \langle 0| Rx(\theta_1)Rz(\theta_2)Rx(\theta_3)$. This is one way to write down the most general qubit effect. Second, the use of a single Rx gate by assigning $\langle w| = \langle 0| Rx(\theta)$, which, with a single parameter, gives a more economical option that is still well-motivated, since an Rx gate can mediate between the $|0\rangle$ and $|1\rangle$ basis states. Let $p_n \in \{3, 1\}$ represent the choice of which of these two options is chosen.

Adjectives are states on two qubits and verbs (only transitive ones appear) are, depending on q_s , states on two or three qubits. For adjectives and verbs, so called *IQP*¹⁴-based states were used. For m qubits this consists of all m qubits initialised in $|0\rangle$, followed by d many IQP layers (Havlíček et al., 2019), where each layer consists of an H gate on every qubit composed with $m - 1$ controlled Rz gates, connecting adjacent qubits. Components (i) and (ii) of Fig. 5 show one IQP layer for a three and a two qubit state, respectively. Motivation for this choice of IQP layers comes – beyond being expressible enough to perform QML (Havlíček et al., 2019) – from the fact that the appearing gates were native to IBMQ’s machines.¹⁵ We considered $d \in \{1, 2\}$, again in order to keep the depth of circuits as small as possible.

For the *RP* task, the relative pronoun ‘that’ is also included in the vocabulary. While at the pregroup level its type depends on whether it is the subject or object case, at the quantum level (noting that $q_s = 0$ for this task) only one kind of quantum state is required. Following the use of Kronecker tensors in (Sadrzadeh et al., 2013, 2014) to model functional

¹⁴Instantaneous Quantum Polynomial.

¹⁵At the time the experiments were run.

<i>MC</i>		<i>RP</i>	
(q_s, p_n, d)	k	(q_s, p_n, d)	k
(1, 1, 1)	22	(0, 1, 1)	114
(1, 1, 2)	35	(0, 1, 2)	168
(1, 3, 1)	40	(0, 3, 1)	234
(1, 3, 2)	53	(0, 3, 2)	288

Table 2: Overview of ansätze studied for the two tasks.

words like relative pronouns, we chose for ‘that’ a GHZ-state, which is displayed in Fig. 6c and which, notably, does not involve any parameters.

Hence, with the laid out approach, the choices that fix an ansatz (with $q_n = 1$ fixed) can be summarised by a triple of hyperparameters (q_s, p_n, d) . The total number k of parameters, denoted $\Theta = (\theta_1, \dots, \theta_k)$, varies correspondingly and depends on the vocabulary. See Table 2 for the ansätze we studied. Note that Fig. 5 shows the circuit of the example sentence from the *MC* task precisely for ansatz (1, 1, 1).

7.2 Model prediction and optimisation

After Step 4, every sentence or phrase P (of type s for *MC* and n for *RP*) is represented by a quantum circuit according to the chosen ansatz. Let the corresponding output quantum state¹⁶ be denoted $|P(\Theta)\rangle$ and define

$$l_{\Theta}^i(P) := \left| \langle i | P(\Theta) \rangle \right|^2 - \epsilon,$$

where $i \in \{0, 1\}$ and ϵ is a small positive number, in our case set to $\epsilon = 10^{-9}$, which ensures that $l_{\Theta}^i(P) \in (0, 1)$ and $l_{\Theta}^0(P) + l_{\Theta}^1(P) \leq 1$, so that

$$l_{\Theta}(P) := \left(l_{\Theta}^0(P), l_{\Theta}^1(P) \right) / \left(\sum_i l_{\Theta}^i(P) \right)$$

defines a probability distribution. The label for P as predicted by the model is then obtained from rounding, i.e. defined to be $L_{\Theta}(P) := \lceil l_{\Theta}(P) \rceil$ with $[0, 1]$ ($[1, 0]$) corresponding to ‘food’ (‘IT’) for the *MC* task and to ‘subject case’ (‘object case’) for the *RP* task.

The *MC* dataset was partitioned randomly into subsets \mathcal{T} (training), \mathcal{D} (development) and \mathcal{P} (testing) with cardinalities $|\mathcal{T}| = 70$, $|\mathcal{D}| = 30$, $|\mathcal{P}| = 30$. Similarly, for the *RP* task with $|\mathcal{T}| = 74$, $|\mathcal{P}| = 31$, but no development set \mathcal{D} , since the ratio of the sizes of vocabulary and dataset did not allow for yet fewer training data, while the overall dataset of 105 phrases could not be easily changed¹⁷. For

¹⁶Generally, a sub-normalised state (in physics jargon).

¹⁷In contrast to the *MC* task, here the data was extracted from an existing dataset, and picking further phrases while ensuring a minimum frequency of all words was non-trivial (see Sec. 6).

both tasks, this was done such that all respective subsets are perfectly balanced with respect to the two classes.

The objective function used for the training is standard cross-entropy; that is, if letting $L(P)$ denote the actual label according to the data, the cost is $C(\Theta) := \sum_{P \in \mathcal{T}} L(P)^T \cdot \log(l_{\Theta}(P))$. For the minimisation of $C(\Theta)$, the SPSA algorithm (Spall, 1998) is used, which for an approximation of the gradient uses two evaluations of the cost function (in a random direction in parameter space and its opposite). The reason for this choice is that in a variational quantum circuit context like here, proper back-propagation requires some form of ‘circuit differentiation’ that would in turn have to be evaluated on a quantum computer – something being actively developed but still unfeasible from a practical perspective. The SPSA approach provides a less effective but acceptable choice for the purposes of these experiments. Finally, no regularisation was used in any form.

7.3 Classical simulation

Owing to the fact that computation with NISQ devices is slow, noisy and limited at the time of writing, it is not practical to do extensive training and comparative analyses on them. This was instead done by using classical calculations to replace Steps 5 and 6 of Fig. 2 in the following sense. For any choice of parameters Θ and some sentence or phrase P , the complex vector $|P(\Theta)\rangle$ can be calculated by simple linear algebra – basically through tensor contraction – and hence the values $l_{\Theta}(P)$, and thereby also the cost $C(\Theta)$ as well as the respective types of errors, can be obtained through a ‘classical simulation’ of the pipeline.

Figs. 7a and 7b present the convergence of the models for the *MC* and *RP* task, respectively, on the training datasets, for the selected sets of ansätze from Table 2. Shown is the cost over SPSA iterations, where each line is from averaging over 20 runs of the optimisation with a random initial parameter point Θ . The reason for this averaging is that there are considerable variances and fluctuations between any individual run due to the crude approximation of the gradient used in the stochastic SPSA algorithm and the specificities of the cost-parameter landscape. As is clear from the plots, the training converges well in all cases. What is more, the dependence of the minima that the average cost converges to on the chosen ansatz reflects the theoretical understanding as follows.

For the *MC* task, the minimum is the lower the

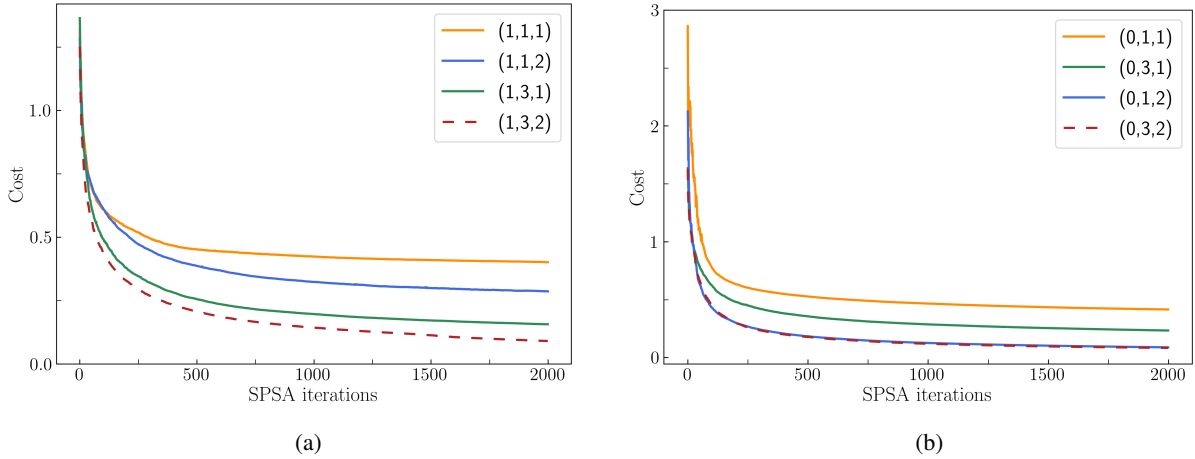


Figure 7: Convergence of the models in the classical simulation (averaged over 20 runs) for different ansätze; in (a) for *MC* task and in (b) for *RP* task.

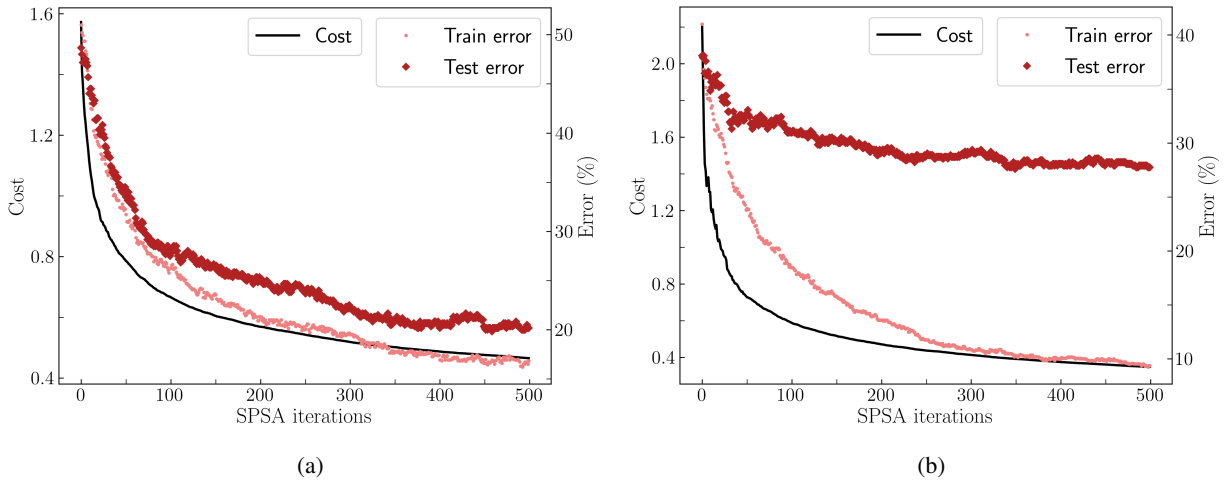


Figure 8: Classical simulation results for the cost and errors (again averaged over 20 runs) in (a) for *MC* task and chosen ansatz (1, 3, 1) and in (b) for *RP* task and chosen ansatz (0, 1, 2).

more parameters. For the *RP* task – being about syntactic structure, essentially about word order – the situation is different but in a way that again is understandable. Given our treatment of ‘that’ (cf. Sec. 7.2), it is not hard to see that the task comes down to learning embeddings such that the verbs’ states become sensitive to which of their two wires connects to the first and the second noun in the phrase, respectively. Hence, the larger d (which fixes the number of parameters for verbs) the lower the minimum.

The plots in Figs. 7a and 7b showcase what is expected from a quantum device if it were noise-free, and if many iterations and runs were feasible time-wise. On that basis, we chose one ansatz per task, that does well with as few parameters as possible, for the actual implementation on quantum hardware: (1, 3, 1) for the *MC* task and (0, 1, 2)

for the *RP* task. Figs. 8a and 8b show simulation results for the correspondingly chosen ansätze together with various errors, but for fewer iterations than in Figs. 7a and 7b for better visibility.

After 500 iterations in the *MC* case, the train and test errors read 16.9% and 20.2%, respectively; in the *RP* case the train and test errors are 9.4% and 27.7%, respectively. Noticeably, the test error for the latter task is somewhat higher than the test error for the former task, as expected from the discussion in Sec. 6. The large vocabulary in combination with the small size of the dataset is one of the most important reasons for this; for example, analysing the data in the aftermath revealed that many of the 115 words in the vocabulary appear only in \mathcal{P} , but not at all in \mathcal{T} .¹⁸

¹⁸More precisely, 17% (36%) of the vocabulary appear zero times (once) in \mathcal{T} .

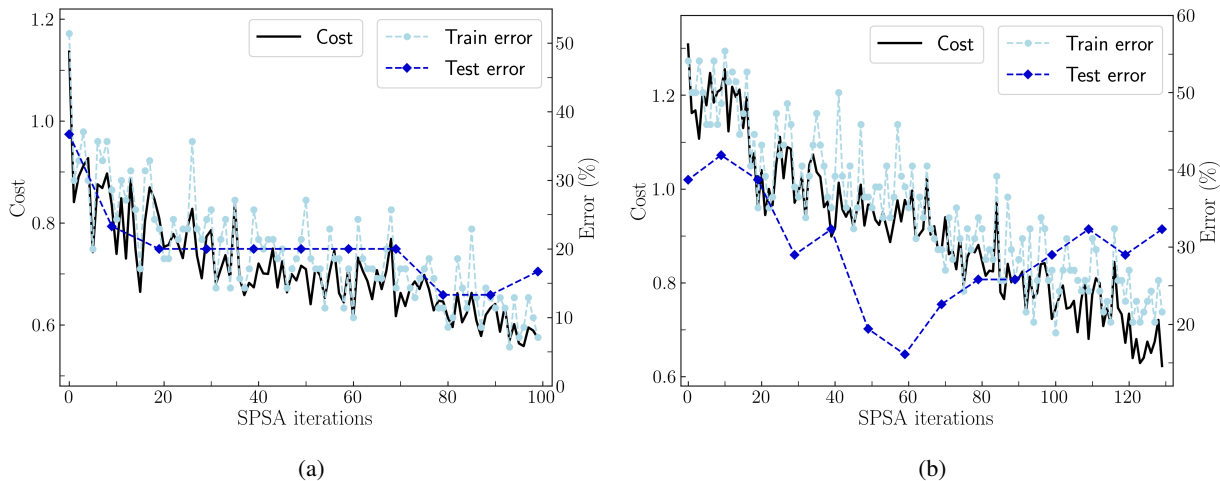


Figure 9: Results from quantum computation for cost and train and test errors (test error for every 10th iteration) in (a) for *MC* task and chosen ansatz (1, 3, 1) and in (b) for *RP* task and chosen ansatz (0, 1, 2).

7.4 Quantum runs

Finally, for the actual experiments on quantum hardware the only missing details are how the definitions from Sec. 7.2 concerning predicted labels, the cost and errors relate to Steps 5 and 6 in Fig. 2. For both experiments, all circuits (compiled with $t|ket\rangle^{TM}$) were run on IBM’s machine `ibmq_bogota`. This is a superconducting quantum computing device with 5 qubits and quantum volume 32.¹⁹

Now, every time the value of the cost or the errors are to be calculated, the compiled circuits corresponding to all sentences or phrases in the corresponding dataset (\mathcal{T} , \mathcal{D} or \mathcal{P}) are sent as a single job to IBM’s device. There, each circuit is run 2^{13} times (the maximum number possible from the machine side). The returned data thus comprises for each circuit (involving q qubits) $2^{13} \times q$ measurement outcomes (0 or 1). For every sentence or phrase P , after appropriately post-selecting the data²⁰(see Secs. 4 and 5), the relative frequencies of outcomes 0 and 1 of the qubit that carries the output state of P , give the estimate of $|\langle i|P(\Theta)\rangle|^2$ (with $i = 0, 1$) and thus of $l_{\Theta}(P)$. The remaining post-processing to calculate the cost or an error is then as for the classical simulation.

The experiments involved one single run of min-

imising the cost over 100 iterations for the *MC* task and 130 iterations for the *RP* task, in each case with an initial parameter point that was chosen on the basis of simulated runs on the train (and dev) datasets.²¹ For the *MC* task, obtaining all the results shown in Fig. 9a took just under 12 hours of run time. This was enabled by having exclusive access to `ibmq_bogota` for this period of time. In contrast, the *RP* jobs were run in IBMQ’s ‘fairshare’ mode, i.e. with a queuing system in place that ensures fair access to the machine for different researchers. As a consequence, for the *RP* task, which is not computationally more involved than the *MC* task, obtaining all the results shown in Fig. 9b took around 72 hours. With access to quantum devices still being a limited resource and ‘exclusive access’ being rationed, we see here the reason for the problems that the time cost of yet larger datasets would entail.

Figures 9a and 9b show the cost and various errors for the *MC* task with ansatz (1, 3, 1) and for the *RP* task with ansatz (0, 1, 2), respectively. Despite the noise levels that come with NISQ era quantum computers, and given the fact of a single run with few iterations compared to the classical simulations in Sec. 7.3, the results look remarkably good – the cost is decreasing with SPSA iterations in both cases, modulo the expected fluctuations. After 100 (130) iterations as reported in Fig. 9a (Fig. 9b), the test error was 16.7% (32.3%) for

¹⁹Quantum volume is a metric which allows quantum computers of different architectures to be compared in terms of overall performance, and it quantifies the largest random circuit of equal width and depth that a quantum computer can successfully implement.

²⁰Note that the *MC* dataset includes sentences that lead to circuits on only three qubits. Here ‘appropriately post-selecting’ means post-selecting two out of the three used qubits.

²¹This choice was made to reduce the chances of being particularly unlucky with the one run that we did on actual quantum hardware. Yet, this choice’s significance should not be overrated given that the influence of quantum noise spoils the predictability of the cost at a particular parameter point from simulated data.

the *MC* and *RP* task, respectively, with F-score 0.85 (0.75). These results were checked to be statistically significant against random guessing with $p \leq 0.001$ for *MC* and $p \leq 0.10$ for *RP* according to a permutation test.

Compared to the simulations (Figs. 8a, 8b), it can be seen that after the same number of iterations, test errors are actually lower for the quantum runs. However, due to the special conditions under which these experiments were performed (single run on quantum hardware subject to quantum noise versus many averaged runs on classical hardware without noise, but with the inherent instability of SPSA optimization still present), such comparisons are not very conclusive. In general, the trends presented in the plots of Figure 9 are the expected based on the size of the datasets. For example, the test error in Fig. 9b shows a paradigmatic example of overfitting around iteration 60.

8 Future work and conclusions

In this work we have provided a detailed exposition of two experiments of NLP tasks implemented on small noisy quantum computers. Our main goal was to present novel larger-scale experiments building on prior proof-of-concept work (Meichanetzidis et al., 2020), while having in mind the NLP practitioner. Despite the prototypical nature of the currently available, albeit rapidly growing in size and quality, quantum processors, we obtain meaningful results on medium-scale datasets. We report that our experiments were successful and converged smoothly, and we conclude that the DISCOCAT framework we have employed is a natural choice for QNLP implementations. We also hope that the current exposition will serve as a useful introduction to practical QNLP for the NLP community.

Having established a QNLP framework for near-term quantum hardware, we briefly outline directions for future work. The ansatz circuits we have used to parameterise the word meanings served well for this work’s goal and also are motivated in the QML literature by the fact that they are conjectured to be hard to simulate classically. However, it was beyond the scope of this work to search for optimal word circuits in a task-specific way. This opens up an exploratory arena for future work on ansätze. In particular, an open question regards trade-offs of performance of ansatz families in a specific task versus general performance on many tasks.

Furthermore, a crucial direction for further work regards scalability. There is more than one way that one can think of scaling-up NLP tasks. What is special to QNLP, is how scaling up in different dimensions manifests itself as a resource cost in the context of quantum computation given the modest quantum devices available today. First of all, we can consider the cost as the sentences get longer. As a sentence scales in length, the number of qubits on which its corresponding quantum circuit is defined, i.e. the circuit width, will scale as well, depending on the number of qubits assigned to each pregroup type. This consideration is remedied by the realisation that quantum computers have been growing in qubit numbers and there is no sign of this growth slowing down. More importantly, however, a longer sentence will incur an exponential time-cost in the number of qubits being post-selected. Note that in the long term, one does not aim to post-select, but employ more sophisticated protocols where only one qubit needs to be measured, resulting in additive approximations of an amplitude encoding a tensor contraction (Arad and Landau, 2010). Of course, in natural language, sentences are usually upper bounded in length and so we can consider these as up-front constant costs.

We can consider two additional ways of scaling up our experiments: the number of sentences, and the size of the vocabulary. A greater number of sentences results in a multiplicative prefactor on the time-cost, which depends only on the time needed to get statistics from the quantum computer for a representative sentence-circuit. As in classical approaches to NLP involving large-scale tasks and big data, in theory we can parallelise the independent evaluations of quantum circuits on multiple quantum processors, repeat jobs in batches on one quantum computer, or run jobs in parallel on many quantum computers to gather more samples and increase the prediction accuracy. However, the current state of available quantum computers does not yet allow for experiments of such magnitude; the runtime of a single circuit is substantial, there are limits to the number of shots and number of circuits submitted in each job, and high-fidelity quantum processors are limited in number which can lead to prohibitive queuing times. Since the quality of quantum hardware is constantly improving, though, such techniques will eventually become valid possibilities.

A larger vocabulary would mean a higher-dimensional parameter space. This motivates the

careful study of the landscapes defined by a task’s cost function, as well as the exploration of other optimisation methods beyond SPSA. Interestingly, this opens up the obvious discussion on a potential quantum advantage in NLP. The type of quantum advantage one hopes to gain over any classical algorithm varies with the problem and would depend on the task at hand. In the NISQ era, a reasonable direction for attempting to establish a quantum advantage is the expressibility of quantum models. There is therefore a need to place both classical and quantum models on equal footing, so that a fair comparison can be made. This can be achieved for example by adopting tools from information geometry (Abbas et al., 2020), rather than just using the naive approach of simply counting variational parameters.

Finally, we remark on the apparent linearity of our model. Indeed, quantum theory is a linear theory, as unitary evolution of pure states makes apparent. However, the subtlety lies in how we chose to embed the input data, in this case the word meanings, and how the cost function is defined in terms of them. The word embeddings are defined as pure quantum states and the cost function is given in terms of outcome probabilities determined by these pure quantum states. Importantly, the Born rule, which gives the probabilities, is a non-linear function of the amplitudes. More generally, quantum machine learning with variational circuits can be viewed elegantly in terms of kernel methods (Schuld and Killoran, 2019; Schuld, 2021). In this light, it becomes clear that the mapping from the parameters defining the input data to the cost is non-linear. Relating to the aforementioned potential quantum advantage in the form of expressibility of quantum models, a possible avenue for obtaining a quantum advantage arises when a QNLP task is designed so that the evaluation of the cost function (or kernel) is hard to simulate classically. These types of quantum advantage in the field of NLP would be meaningful in that they would be examples of non-contrived real-world applications of quantum computers in the near-term.

Acknowledgments

We are grateful to Richie Yeung for his help on technical issues, and also, along with Alexis Toumi, for DISCOPY support. We also thank Marcello Benedetti for helpful discussions. We would furthermore like to thank CQC’s $t|ket\rangle^{TM}$ team for support with `pytket`. We acknowledge the use of

IBM Quantum services for this work. The views expressed are those of the authors, and do not reflect the official policy or position of IBM or the IBM Quantum team.

References

- Amira Abbas, David Sutter, Christa Zoufal, Aurélien Lucchi, Alessio Figalli, and Stefan Woerner. 2020. [The Power of Quantum Neural Networks](#).
- S. Abramsky and B. Coecke. 2004. A Categorical Semantics of Quantum Protocols. In *Proceedings of the 19th Annual IEEE Symposium on Logic in Computer Science*, pages 415–425. IEEE Computer Science Press. arXiv:quant-ph/0402130.
- Itai Arad and Zeph Landau. 2010. [Quantum Computation and the Evaluation of Tensor Networks](#). *SIAM Journal on Computing*, 39(7):3089–3121.
- Dea Bankova, Bob Coecke, Martha Lewis, and Dan Marsden. 2019. Graded Entailment for Compositional Distributional Semantics. *Journal of Language Modelling*, 6(2):225–260.
- Ivano Basile and Fabio Tamburini. 2017. [Towards Quantum Language Models](#). In *Proceedings of the 2017 Conference on Empirical Methods in Natural Language Processing*, pages 1840–1849, Copenhagen, Denmark. Association for Computational Linguistics.
- Johannes Bausch, Sathyawageeswar Subramanian, and Stephen Piddock. 2020. [A Quantum Search Decoder for Natural Language Processing](#).
- Kerstin Beer, Dmytro Bondarenko, Terry Farrelly, Tobias J. Osborne, Robert Salzmann, Daniel Scheiermann, and Ramona Wolf. 2020. [Training Deep Quantum Neural Networks](#). *Nature Communications*, 11.
- Marcello Benedetti, Erika Lloyd, Stefan Sack, and Mattia Fiorentini. 2019. [Parameterized Quantum Circuits as Machine Learning Models](#). *Quantum Science and Technology*, 4(4):043001.
- Kishor Bharti, Alba Cervera-Lierta, Thi Ha Kyaw, Tobias Haug, Sumner Alperin-Lea, Abhinav Anand, Matthias Degroote, Hermanni Heimonen, Jakob S. Kottmann, Tim Menke, Wai-Keong Mok, Sukin Sim, Leong-Chuan Kwek, and Alán Aspuru-Guzik. 2021. [Noisy Intermediate-Scale Quantum \(NISQ\) Algorithms](#).
- Benjamin J. Brown, Daniel Loss, Jiannis K. Pachos, Chris N. Self, and James R. Wootton. 2016. [Quantum Memories at Finite Temperature](#). *Reviews of Modern Physics*, 88(4).
- Y. Cao, J. Romero, and A. Aspuru-Guzik. 2018. [Potential of Quantum Computing for Drug Discovery](#). *IBM Journal of Research and Development*, 62(6):6:1–6:20.

- Yudong Cao, Jonathan Romero, Jonathan P. Olson, Matthias Degroote, Peter D. Johnson, Mária Kieferová, Ian D. Kivlichan, Tim Menke, Borja Peropadre, Nicolas P. D. Sawaya, Sukin Sim, Libor Veis, and Alán Aspuru-Guzik. 2019. [Quantum Chemistry in the Age of Quantum Computing](#). *Chemical Reviews*, 119(19):10856–10915.
- Yiwei Chen, Yu Pan, and Daoyi Dong. 2020. [Quantum Language Model with Entanglement Embedding for Question Answering](#).
- Bob Coecke, Giovanni de Felice, Konstantinos Meichanetzidis, and Alexis Toumi. 2020. [Foundations for Near-Term Quantum Natural Language Processing](#).
- Bob Coecke and Aleks Kissinger. 2017. [Picturing Quantum Processes: A First Course in Quantum Theory and Diagrammatic Reasoning](#). Cambridge University Press.
- Bob Coecke, Mehrnoosh Sadrzadeh, and Stephen Clark. 2010. Mathematical Foundations for a Compositional Distributional Model of Meaning. *Linguistic Analysis*, 36:345–384.
- Giovanni de Felice, Alexis Toumi, and Bob Coecke. 2020. DisCoPy: Monoidal Categories in Python. In *Proceedings of the 3rd Annual International Applied Category Theory Conference*. EPTCS.
- Angel J. Gallego and Roman Orus. 2019. [Language Design as Information Renormalization](#).
- Edward Grefenstette and Mehrnoosh Sadrzadeh. 2011. Experimental Support for a Categorical Compositional Distributional Model of Meaning. In *Proceedings of the Conference on Empirical Methods in Natural Language Processing*, pages 1394–1404. Association for Computational Linguistics.
- Sanjay Gupta and R.K.P. Zia. 2001. [Quantum Neural Networks](#). *Journal of Computer and System Sciences*, 63(3):355–383.
- Vojtěch Havlíček, Antonio D Córcoles, Kristan Temme, Aram W Harrow, Abhinav Kandala, Jerry M Chow, and Jay M Gambetta. 2019. Supervised Learning with Quantum-Enhanced Feature Spaces. *Nature*, 567(7747):209–212.
- Dimitri Kartsaklis and Mehrnoosh Sadrzadeh. 2014. A Study of Entanglement in a Categorical Framework of Natural Language. In B. Coecke, I. Hasuo, and P. Panangaden, editors, *Quantum Physics and Logic 2014 (QPL 2014)*. EPTSC 172, pages 249–261.
- Dimitri Kartsaklis, Mehrnoosh Sadrzadeh, and Stephen Pulman. 2012. A Unified Sentence Space for Categorical Distributional-Compositional Semantics: Theory and Experiments. In *COLING 2012, 24th International Conference on Computational Linguistics, Proceedings of the Conference: Posters, 8-15 December 2012, Mumbai, India*, pages 549–558.
- Dimitri Kartsaklis, Mehrnoosh Sadrzadeh, Stephen Pulman, and Bob Coecke. 2016. [Reasoning about Meaning in Natural Language with Compact Closed Categories and Frobenius Algebras](#), Lecture Notes in Logic, page 199–222. Cambridge University Press.
- J. Lambek. 2008. *From Word to Sentence*. Polimetrica, Milan.
- Martha Lewis. 2019. Modelling Hyponymy for DisCoCat. In *Proceedings of the Applied Category Theory Conference*, Oxford, UK.
- Konstantinos Meichanetzidis, Alexis Toumi, Giovanni de Felice, and Bob Coecke. 2020. [Grammar-Aware Question-Answering on Quantum Computers](#).
- Michael A. Nielsen and Isaac L. Chuang. 2011. *Quantum Computation and Quantum Information: 10th Anniversary Edition*, 10th edition. Cambridge University Press, New York, NY, USA.
- Lee J O’Riordan, Myles Doyle, Fabio Baruffa, and Venkatesh Kannan. 2020. [A Hybrid Classical-Quantum Workflow for Natural Language Processing](#). *Machine Learning: Science and Technology*, 2(1):015011.
- Robin Piedeleu, Dimitri Kartsaklis, Bob Coecke, and Mehrnoosh Sadrzadeh. 2015. Open System Categorical Quantum Semantics in Natural Language Processing. In *Proceedings of the 6th Conference on Algebra and Coalgebra in Computer Science*, Nijmegen, Netherlands.
- S. Pirandola, U. L. Andersen, L. Banchi, M. Berta, D. Bunandar, R. Colbeck, D. Englund, T. Gehring, C. Lupo, C. Ottaviani, and et al. 2020. [Advances in Quantum Cryptography](#). *Advances in Optics and Photonics*, 12(4):1012.
- H. Ramesh and V. Vinay. 2003. [String Matching in \$O\(n+m\)\$ Quantum Time](#). *Journal of Discrete Algorithms*, 1(1):103–110. Combinatorial Algorithms.
- Laura Rimell, Jean Maillard, Tamara Polajnar, and Stephen Clark. 2016. [RELPRON: A Relative Clause Evaluation Data Set for Compositional Distributional Semantics](#). *Computational Linguistics*, 42(4):661–701.
- Mehrnoosh Sadrzadeh, Stephen Clark, and Bob Coecke. 2013. The Frobenius Anatomy of Word Meanings I: Subject and Object Relative Pronouns. *Journal of Logic and Computation*, 23(6):1293–1317.
- Mehrnoosh Sadrzadeh, Stephen Clark, and Bob Coecke. 2014. The Frobenius Anatomy of Word Meanings II: Possessive Relative Pronouns. *Journal of Logic and Computation*, 26(2):785–815.
- Mehrnoosh Sadrzadeh, Dimitri Kartsaklis, and Esma Balkir. 2018. Sentence Entailment in Compositional Distributional Semantics. *Annals of Mathematics and Artificial Intelligence*, 82:189–218.

- Maria Schuld. 2021. [Quantum Machine Learning Models are Kernel Methods](#).
- Maria Schuld and Nathan Killoran. 2019. Quantum Machine Learning in Feature Hilbert Spaces. *Physical review letters*, 122(4):040504.
- Seyon Sivarajah, Silas Dilkes, Alexander Cowtan, Will Simmons, Alec Edgington, and Ross Duncan. 2020. $t|ket\rangle$: a Retargetable Compiler for NISQ Devices. *Quantum Science and Technology*, 6(1):014003.
- J. C. Spall. 1998. [Implementation of the Simultaneous Perturbation Algorithm for Stochastic Optimization](#). *IEEE Transactions on Aerospace and Electronic Systems*, 34(3):817–823.
- Nathan Wiebe, Alex Bocharov, Paul Smolensky, Matthias Troyer, and Krysta M Svore. 2019. [Quantum Language Processing](#).
- William Zeng and Bob Coecke. 2016. [Quantum Algorithms for Compositional Natural Language Processing](#). *Electronic Proceedings in Theoretical Computer Science*, 221:67–75.